Copyright © 2006 American Scientific Publishers
All rights reserved
Printed in the United States of America

Journal of
Nanoscience and Nanotechnology
Vol. 6, 1662–1666, 2006

Syntheses of Ag, PbSe, and PbTe Nanocrystals and Their Binary Self-Assembly Exploration at Low Size-ratio

Weigang Lu[1], Jiye Fang[1,*], Jun Lin[2], Jun Zhang[1], Zhaoyong Sun[1], and Kevin L. Stokes[3]

[1] *Department of Chemistry and Advanced Materials Research Institute, University of New Orleans, New Orleans, LA 70148, USA*
[2] *Key Laboratory of Rare Earth Chemistry and Physics, Changchun Institute of Applied Chemistry, Chinese Academy of Sciences, Changchun, Jilin 130022, P. R. China*
[3] *Department of Physics and Advanced Materials Research Institute, University of New Orleans, New Orleans, LA 70148, USA*

Nanocrystals of Ag, PbSe, and PbTe were prepared via a high-temperature organic solution approach, respectively. Using a size-selection technique, the size-distribution of each set of nanocrystals could be fine-tuned and finally monodisperse products were achieved. Superlattice structure of binary self-assemblies in low size-ratio were also explored and characterized by transmission electron microscopy. It is realized that a success of achieving binary self-assembly pattern is greatly dependent on several key factors including particle size-distributions, relative concentrations of both components, as well as the size-ratios between Ag and PbSe (or PbTe) nanocrystals.

Keywords: Binary Self-Assembly, Nanocrystal, Monodisperse, Ag, PbSe, Size-Ratio, Size-Selection.

1. INTRODUCTION

Exploration of binary self-assembly may create alternative avenue to develop advanced nanomaterials which provide novel multi-functional properties. Binary nanocrystalline superlattice consists of two sets of high-quality nanocrystals (NCs) with a certain size-ratio and optimal relative concentrations. The superlattice structures of binary self-assembly which were extensively investigated are AB_2 [1,2] and AB_{13}.[2,3] Murray and Sanders[4] suggested that the AB_2 assembled pattern should only be stable in the size-ratio ranges of $0.482 < R_B/R_A < 0.624$ (R is diameter of particles A or B). Furthermore, it has been reported that it could also result in an AB_{13} structure when the size-ratio of two sets of components approaches to ~0.565–0.58.[3,5–6] We have an interest in exploring the binary close-packed structure when the size-ratio reduces to less than 0.4. This investigation is inspired because of the fact that in most syntheses and size-refinement processes, the monodisperse NCs may companied with some extreme small particles, and it is essential and interesting to study their influence on the self-assembled structures of the selected NCs.

2. EXPERIMENTAL DETAILS

All of the chemicals were used as received from Aldrich without further purification, unless otherwise specify.

2.1. Synthesis of Ag Nanocrystals

High-quality Ag NCs were previously prepared by Harfenist et al. using an aerosol processing approach.[7] In our typical experiment, 0.1667 g of silver acetate (AgAc, 99.999%) and 3.0 mL of oleic acid (90%) were combined with 15 mL of benzyl ether in a three-neck flask equipped with a condenser. The system was rapidly heated to 200 °C under argon stream and this vigorously stirred mixture was maintained at 200 °C for additional 20 min. As the temperature increases, the color of the solution gradually turned dark-red, indicating a formation of Ag NCs. These Ag colloids were cooled to room temperature by quickly removing the heating source, and then isolated by adding a sufficient amount of ethanol (99.5%, Aaper Alcohol and Chemical Co.) and separating with centrifugation. The

*Author to whom correspondence should be addressed.

 1533-4880/2006/6/1662/005 doi:10.1166/jnn.2006.228

yielded precipitate was re-dispersed in hexane (99%) followed by a size-selection treatment.

2.2. Synthesis of PbSe Nanocrystals

The synthesis approach of PbSe NCs is based on a procedure developed by Murray et al.[8,9] using a similar device. Typically, 1.081 g of lead acetate [$Pb(Ac)_2 \cdot 3H_2O$, 99.999%] was added into 15 mL of phenyl ether (99%) in the presence of 3.6 mL of oleic acid (90%) with constant agitation. The mixture was heated up to 150 °C under flowing argon, remained for 30 min, and then cooled to room temperature. Under argon atmosphere, such cold solution was subsequently mixed with 8 mL of Se-TOP solution (1 M for Se) which was pre-prepared by dissolving metal selenium (99.99%) into trioctylphosphine (TOP, 90%) in a glovebox, and rapidly injected 15 mL of hot phenyl ether which was heated to 180 °C under argon stream on a Schlenk line. The hot mixture was vigorously stirred for 6 min and the resulting PbSe NCs were collected and size-selected using a similar method as mentioned above.

2.3. Synthesis of PbTe Nanocrystals

The Synthesis of PbTe NCs is similar to that of PbSe NCs and it can be referred to Lu's work[10] Firstly, Te-TOP solution (0.5 M for Te) was pre-prepared as Te-source by adding 6.38 g of tellurium shot (99.999%) into 100 mL of TOP in a glovebox and stirring for overnight. The yellow mixture was eventually heated to 150 °C under Ar atmosphere for 5 mins to ensure the formation of a clear stock solution. Secondly, 1.081 g of lead acetate trihydrate, 3.0 mL of oleic acid and 15 mL of phenyl ether were mixed and heated to 150 °C for 20 min under argon atmosphere. After the solution was cooled to 40 °C, it was transferred into a glovebox and mixed with 5.7 mL of TOP-Te stock solution in a cool-bath of ~10 °C. This low-temperature mixed solution was then rapidly injected into vigorous stirred phenyl ether (15 mL) that was pre-heated to 200 °C in a three-neck flask equipped with a condenser under argon stream. After the injection, the temperature of the mixture dropped to ~115 °C. Once the reaction temperature picked up to 200 °C in ~5 min, the crystalline growth was terminated by an immediate removal of the heating source. Finally, a size-selective precipitation was conducted by centrifugation using a pair of solvents consisting of hexane and ethanol.

2.4. Characterization

The phase structure was analyzed using X-ray diffraction (XRD) carried out on a Philips X-pert system with Cu K_α radiation ($\lambda = 0.15405$ nm). The morphology of NCs and the image of self-assembled pattern were examined using a transmission electron microscope (TEM, JEOL 2010). In addition to TEM observation, size distribution of NCs was also measured using a light scattering technique (DynaPro 99 Molecular Sizing Instrument). The optical absorption was recorded using a Cary UV-Vis spectrophometer (Cary Varian Optical Spectroscopy Instruments).

3. RESULTS AND DISCUSSION

As stated above, all of the as-synthesized NCs were refined through additional size-selection, i.e., a size-sorting treatment. In solution, NCs are stable with respect to aggregation only if capping ligands provide a repulsive force of sufficient strength and range to counteract the inherent van der Waals attraction between NCs. Size-selective precipitation involves the titration of a nonsolvent into the dispersion and centrifugation. In this work, a pair of solvents consisting of hexane and ethanol was employed. Self-assembly is based on a similar mechanism and involves a preferential evaporation of solvent from a mixed solvent/nonsolvent system (e.g., the hexane/hexanol system) to bring about gradual flocculation. The energy barrier to agglomeration provided by the capping ligand is determined by the energy of mixing of the capping ligand in the solvent. Assembled NC layer(s) can be prepared by adjusting the solvent composition to keep the NC dispersion stable as it is concentrated by the evaporation of the solvent.

Ag NCs were prepared and sorted into different monodisperse samples with various sizes after a size-selection treatment. Figure 1(a) displays the XRD traces recorded on these Ag NCs in different sizes. According to the standard ICDD PDF card (No. 03-0931), all of the three detected peaks are indexed as those from the bulk silver specimen, indicating that they are well-defined cubic structure with *Fm3m* (225) space group ($a = 4.067$ Å). The order of the crystalline sizes for the three samples are estimated in a sequence of "$a > b > c$," by applying the Scherrer equation[11] to the line broadening of the peak (111). Figure 1(b) presents UV absorption spectra, showing a very slight blue-shift for smaller size crystals.

Figure 2(a) shows a transmission electron micrograph (TEM) image (sample c), illustrating size, morphology and self-assembled pattern of Ag NCs. It exhibits high-quality Ag NCs with a spherical morphology. The average diameter of these Ag NCs were measured as ~4.2 ± 0.7 nm on the basis of the TEM image. By properly adjusting the solvent ratio between hexane and hexanol as well as the concentration of Ag NCs, we demonstrate that it is possible to achieve monolayer self-assembled pattern with hexagonal-close-packed alignment and a remarkable degree of long-range order. The average spacing between Ag and Ag NCs was determined as approximately 3.0 nm, and it is believed that this space should be filled by the residues of oleic acid coated on the surface of Ag NC surface.[12] Figure 2(b) presents a TEM image of close-packed PbSe NCs, implying that the PbSe NCs assemble into a two-dimensional monolayer with local hexagonal order. Based on this TEM observation, the average size of these quasi-monodisperse PbSe NCs was also estimated

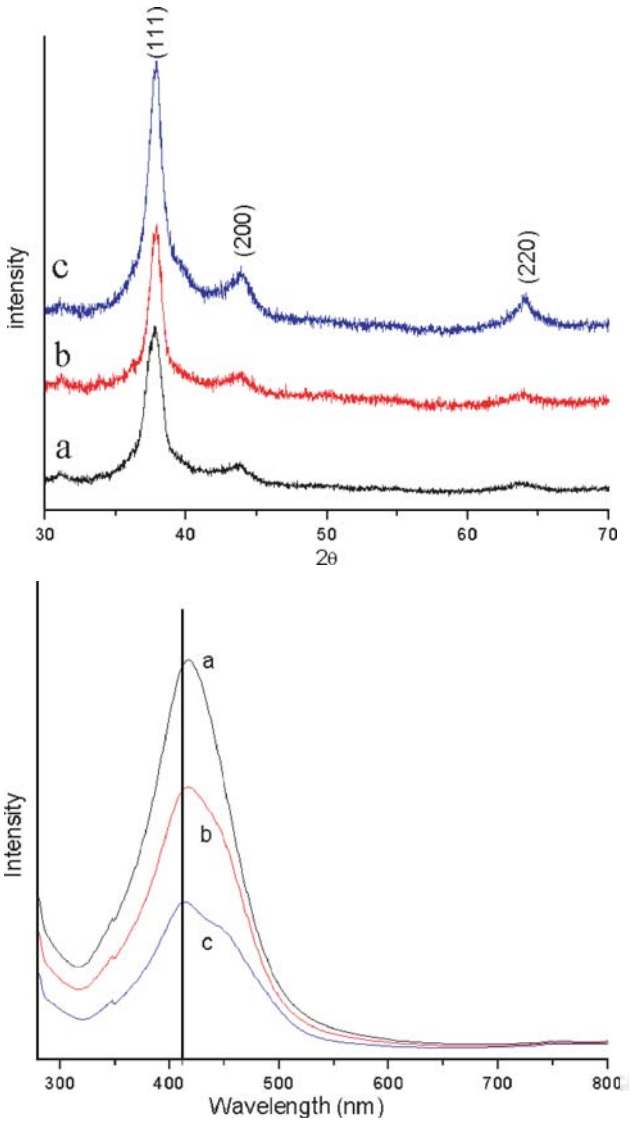

Fig. 1. (A, top) X-ray diffraction pattern of Ag nanocrystals in different sizes (samples a, b, and c); (B, bottom) UV-Vis absorption spectra of Ag nanocrystals (samples a, b, and c).

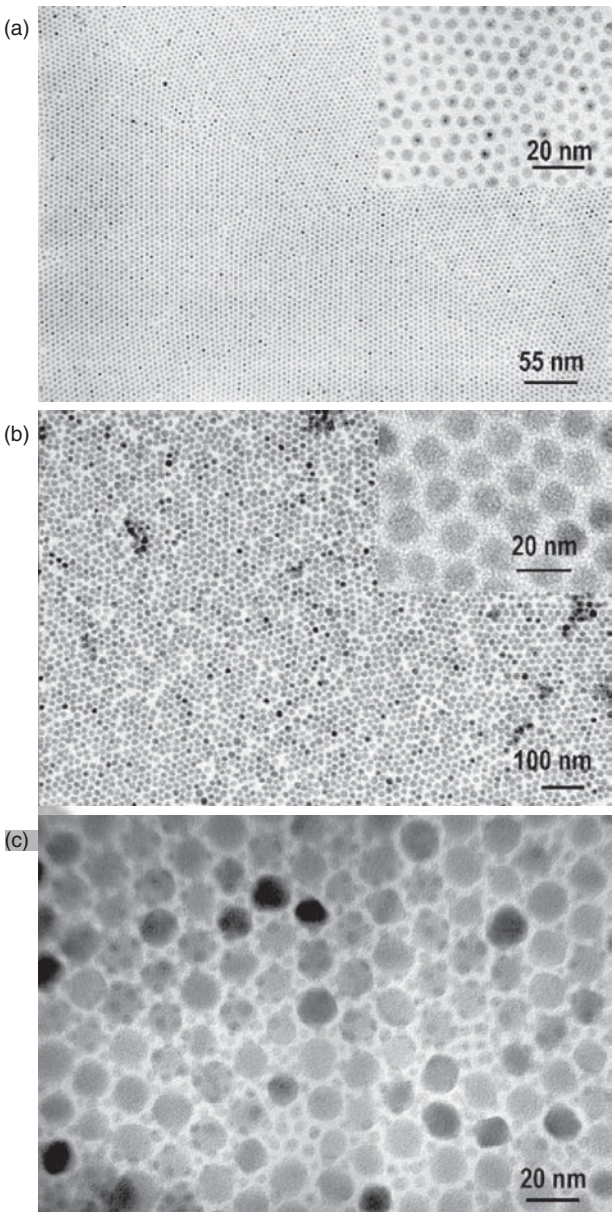

Fig. 2. (a) TEM image of 4.2-nm Ag NC self-assembly pattern; (b) TEM image of 13-nm PbSe NC self-assembly pattern; (c) TEM image of 4.2-nm Ag/13-nm PbSe binary self-assembly pattern at size-ratio 0.32.

as $\sim 13 \pm 0.9$ nm, whereas the minimum spacing between PbSe and PbSe NCs approximately 3.6 nm. The difference of NC-NC average spacing between Ag system and PbSe system is probably because of different crystalline size between both systems. As expected, smaller particles form a denser ordered pattern than larger particles do if other conditions such as NC concentration are maintained similar. In the situation of PbSe NCs, relatively broadening size distribution may also result in a low-quality assembly-pattern, giving larger particle-particle spacing. The characteristics of PbSe NCs have been well-investigated in previous reports,[8, 9, 13, 14] Kiely et al.[1] determined that a superlattice structure of AB_2 could be observed when both sets of components containing spherical Au NCs of larger particles A (7.8 nm in diameter) and smaller particles B (4.5 nm in diameter) with a radius-ratio $R_B/R_A \approx 0.58$. Similar AB_2 structure was also determined by Murray et al.[2] when 11-nm γ-Fe_2O_3 NCs and 6.3-nm PbSe NCs were used for self-assembly in a radius-ratio of 0.55–0.58. Moreover, they also found that an AB_{13} superlattice structure could be achieved at the radius-ratio $R_B/R_A \approx 0.55$ when the size-ratios between PbSe and γ-Fe_2O_3 NCs were tuned from 0.4 to 0.7. As mentioned in the section of introduction, we have an interest in examining the possible self-assembled structure when the size-ratio moves to less than 0.4. Figure 2(c) presents a binary NC assemblies containing a mixture of Ag NCs (sample c, 4.2 nm) and PbSe NCs (13 nm) while their relative concentrations were properly adjusted (we prepared the sample for a target structure of AB_{13}, i.e., PbSe:Ag $\approx 1:13$). With a size-ratio of $R_{Ag}/R_{PbSe} \approx 0.32$ in our case, the TEM image still

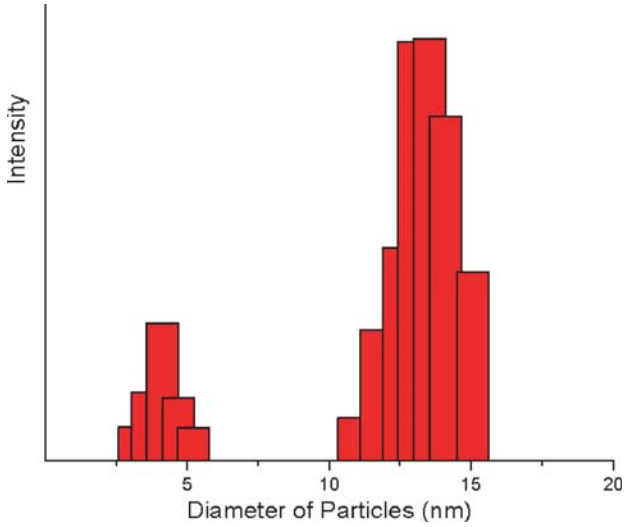

Fig. 3. Crystalline size distribution of binary 4.2-nm Ag/13-nm PbSe NC system determined by light scattering technique.

exhibits a hexagonally ordered PbSe backbone assembly although a few of defects could be detected. However, the Ag nanoparticles tended to surround each unit of PbSe particle, forming 3D structure based on monolayer of PbSe assembly. In order to verify the relative crystalline sizes of both sets of components, a light scattering investigation on this mixed sample was also conducted. As presented in Figure 3, the result from light scattering is in a good agreement with those measured from TEM images.

The relative concentrations of both sets of components are also one of the significant parameters which control the formation of ordered superlattice structure. Figure 4(a) shows a monolayer pattern of 11-nm PbTe NCs. Figure 4(b) is a binary NC assemblies of 4.2-nm Ag NCs and 11.4-nm PbTe NCs ($R_{Ag}/R_{PbTe} \approx 0.36$) with a relative concentration ratio of PbTe:Ag $\approx$ 1:2, showing a disorder structure for both sets of NCs, and the component of PbTe NCs even loses its orientational order in this case. This observation implies that the relative concentrations of both colloidal particles may be the second key parameters in binary self-assembly, after the factors of size-ratio between two sets of components and size-distribution.

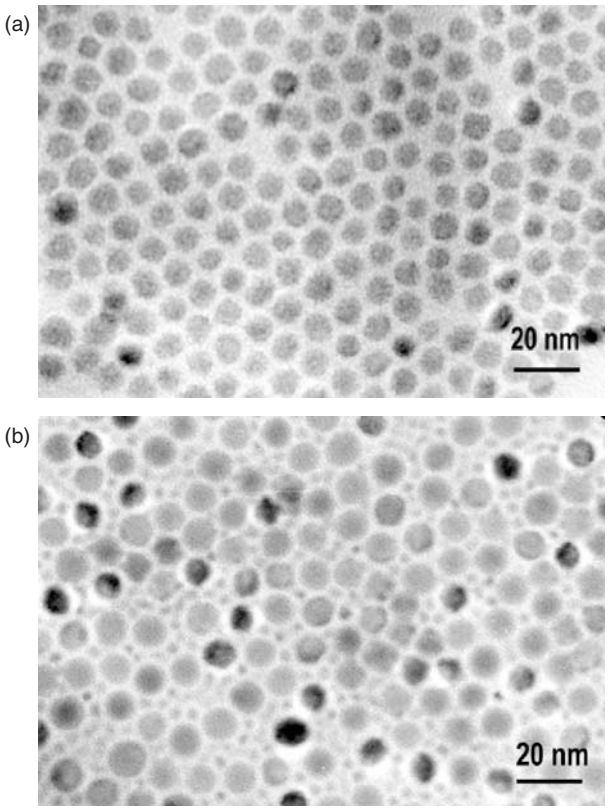

Fig. 4. (a) TEM image of 11.4-nm PbTe NC self-assembly pattern; (b) TEM image of monolayer pattern containing 4.2-nm Ag NCs and 11.4-nm PbTe NCs.

4. CONCLUSIONS

Monodisperse, high-quality of Ag NCs were successfully prepared and refined by employing high-temperature organic solution synthetic approach and polar/non-polar solvent size-selection post-treatment, respectively. Self-assembled patterns of each single component, including Ag NCs, PbSe NCs, and PbTe NCs were also demonstrated in this paper. Initial exploration of low size-ratio of binary assembly was conducted. It is anticipated that

(1) at low size-ratio system (e.g., $R_B/R_A < 0.4$), it is still possible to achieve orientationally ordered assembly pattern of the large-size particle-component set;
(2) the successful arrangement of the second set of component (small-size particles) is greatly depending on the relative concentrations of both colloids;
(3) size-distribution of each component is also alternative key factor to ensure the success of binary self-assembly.

In order to achieve the defined binary-structural self-assembly, performance of further investigations is still required.

Acknowledgments: This work was supported by NSF CAREER Program (DMR-0449580), NSF NER program (DMI-0508412) and DARPA HR0011-05-1-0031. Prof. Fang gratefully thanks Prof. Timothy Hughbanks and Chemistry Department/Texas A&M University for rapid acceptance during his displacement caused by hurricane Katrina. Professor Lin is grateful for the financial support by the MOST of China (2003CB314707), the NSFC 00310530, 50225205, and 20431030.

References and Notes

1. C. J. Kiely, J. Fink, M. Brust, D. Bethell, and D. J. Schiffrin, *Nature* 396, 444 (**1998**).
2. F. X. Redl, K.-S. Cho, C. B. Murray, and S. O'Brien, *Nature* 423, 968 (**2003**).

3. E. V. Shevchenko, D. V. Talapin, S. O'Brien, and C. B. Murray, *J. Am. Chem. Soc.* 127, 8741 **(2005)**.
4. M. J. Murray and J. V. Sanders, *Phil. Mag. A* 42, 721 **(1980)**.
5. P. Bartlett, R. H. Ottewill, and P. N. Pusey, *Phy. Rev. Lett.* 68, 3801 **(1992)**.
6. M. D. Eldridge, P. A. Madden, and D. Frenkel, *Nature* 365, 35 **(1993)**.
7. S. A. Harfenist, Z. L. Wang, M. M. Alvarez, I. Vezmar and R. L. Whetten, *J. Phys. Chem.* 100, 13904 **(1996)**.
8. C. B. Murray, S. Sun, W. Gaschler, T. A. Betley, and C. R. Kagan, *J. Res. Dev.* 45, 47 **(2001)**.
9. F. Chen, K. L. Stokes, W. Zhou, J. Fang, and C. B. Murray, *Mat. Res. Soc. Symp. Proc.* 691, 359 **(2002)**.
10. W. Lu, J. Fang, K. L. Stokes, and J. Lin, *J. Am. Chem. Soc.* 126, 11798 **(2004)**.
11. H. P. Klug and L. E. Alexander, *X-ray Differaction Procedure for Polycrystalline and Amorphous Materials*, Wiley, New York **(1954)**, p. 512.
12. S. Sun and C. B. Murray, *J. Appl. Phys.* 85, 4325 **(1999)**.
13. K.-S. Cho, D. V. Talapin, W. Gaschler, and C. B. Murray, *J. Am. Chem. Soc.* 127 7140 **(2005)**.
14. W. Lu, J. Fang, Y. Ding, and Z. L. Wang, *J. Phys. Chem. B* 109, 19219 **(2005)**.

Received: 5 October 2005. Accepted: 5 December 2005.